Effect of Ni and vacancy concentration on initial formation of Cu precipitate in Fe–Cu–Ni ternary alloys by molecular dynamics simulation*

Ke Liu(刘珂), Li-Juan Hu(胡丽娟)†, Qiao-Feng Zhang(张巧凤), Yao-Ping Xie(谢耀平), Chao Gao(高超), Hai-Ying Dong(董海英), and Wan-Yi Liang(梁婉怡)

Key Laboratory for Microstructures and Institute of Materials Science, School of Materials Science and Engineering, Shanghai University, Shanghai 200072, *China*

(Received 13 January 2017; revised manuscript received 4 May 2017; published online 20 June 2017)

In the present work, the effects of Ni atoms and vacancy concentrations (0.1%, 0.5%, 1.0%) on the formation process of Cu solute clusters are investigated for Fe–1.24%Cu–0.62%Ni alloys by molecular dynamics (MD) simulations. The presence of Ni is beneficial to the nucleation of Cu precipitates and has little effect on coarsening rate in the later stage of aging. This result is caused by reducing the diffusion coefficient of Cu clusters and the dynamic migration of Ni atoms. Additionally, there are little effects of Ni on Cu precipitates as the vacancy concentration reaches up to 1.0%, thereby explaining the embrittlement for reactor pressure vessel (RPV) steel. As a result, the findings can hopefully provide the important information about the essential mechanism of Cu cluster formation and a better understanding of ageing phenomenon of RPV steel. Furthermore, these original results are analyzed with a simple model of Cu diffusion, which suggests that the same behavior could be observed in Cu-containing alloys.

Keywords: Cu precipitates, vacancy concentration, Fe–Cu–Ni alloys, molecular dynamics

PACS: 36.40.–c, 61.82.Bg, 02.70.Ns **DOI:** 10.1088/1674-1056/26/8/083601

1. Introduction

The nucleation and growth of Cu-rich clusters have been proved to play an important role in the microstructural and mechanical properties in RPV steel. Dislocation glide is impeded and yield strength is increased due to the formation of Cu clusters, which leads to the embrittlement in RPV steel.[1,2] The continuous irradiation by fast neutrons causes a super-saturation of vacancies and self-interstitials and enhances the diffusion of Cu, which occurs via the vacancy mechanism. Over the last sixty years, Cu precipitates have been extensively studied in experiment and theory. In the experimental aspect, small-angle x-ray neutron scattering,[3] transmission electron microscopy (TEM),[4,5] atom probe tomography (APT),[6,7] etc. have been utilized to analyze the structural, compositional, and morphological evolutions of Cu precipitates.[8–15] In the theoretical aspect, multi-scale simulations have been performed to study the formation and evolution of Cu-rich clusters or precipitates, phase transition, Cu diffusion in α-Fe[16–22] and interactions between Cu clusters and vacancies.[23–33]

Investigations have shown that Cu nano-clusters may consist of not only pure Cu but also complexes, such as Cu_mNi_n clusters,[29,31] which have the lower formation energies than that of pure Cu cluster.[19,34] In general, the literature data show that the main function of Ni atoms in the Cu-contained ferric alloys can accelerate the precipitation of Cu clusters[35–37] and increase the quantity of Cu clusters[38] during ageing. High vacancy concentration can also increase Cu clusters precipitating.[39] However, according to Wang *et al.*'s study,[40] Ni atom has a temporal delay effect on Cu precipitate with a specific behavior of inhibiting Cu precipitation during ageing, which is poorly explained. Moreover, recently published calculations only focus on the influence of vacancy concentration or Ni atom on Cu precipitate, and few studies show consideration of the interaction between vacancy concentration and Ni atom for Cu precipitate on an atomic scale.

In the present work, MD simulations are employed to investigate the influences of vacancy concentration and Ni atom on the formation process of Cu solute cluster in Fe–Cu–Ni ternary alloy. The diffusion coefficient as well as the size of Cu cluster is calculated to evaluate the Cu diffusivity. Results of Fe–Cu–Ni alloy and Fe–Cu alloy under different vacancy concentrations are compared to explain the promotion and inhibition effect of Ni atom on Cu precipitation with ageing time increasing. Ni atoms accelerate Cu precipitation at the nucleation stage, while inhibit Cu precipitation at the coarsening stage. Moreover, for the alloy with 1.0% vacancy concentration, Ni atoms, compared with vacancy concentration, have little effect on Cu diffusion. These results provide important information about essential mechanism for Cu enriched cluster

*Project supported by the National Natural Science Foundation of China (Grant No. 51301102) and the Science and Technology Commission of Shanghai Municipality, China (Grant No. 15ZR1416000).

†Corresponding author. E-mail: lijuanhu@shu.edu.cn

© 2017 Chinese Physical Society and IOP Publishing Ltd

formation to understand ageing phenomenon of RPV steel.

2. Molecular dynamics simulation details

The MD simulations are carried out by using the large-scale atomic molecular massively parallel simulator (LAMMPS) code.[40,41] For metals, the interaction between atoms are typically described by the embedded-atom method (EAM) potential. The Fe–Cu–Ni EAM potential,[35] which is well suitable for the present study, is employed to describe the alloy thermodynamic properties and the interactions between solute atoms and point defects. The equilibrium solubility of Cu in Fe-matrix, obtained through this potential agrees well with the experimental value.

Cu clusters in Fe–1.24%Cu–0.62%Ni (Fe–Cu–Ni) alloys with vacancy concentrations of 0.1% (0.1%v), 0.5% (0.5% v), and 1.0% (1.0% v), and in Fe–1.24%Cu (Fe–Cu) alloys with vacancy concentrations of 0.1% (0.1% v) and 1.0% (1.0% v) have been studied at 773 K. All percentages mentioned in this paper are atomic percentages unless otherwise stated. The vacancy concentration values of about 0.1% to 1.0% adopted in this paper are necessary, because otherwise MD simulations would be too slow. According to previous studies,[42] the vacancy concentration range is rational, which does not change the Cu cluster formation mechanism. A cubic simulation cell containing the bcc-Fe lattice with x direction, y direction, and z direction parallel to the [100], [010], and [001] axes is constructed. The dimensions of the cube are $35a \times 35a \times 35a$ (85750 lattice sites), where a is the lattice constant ($a = 2.855$ Å) of bcc-Fe. Three-dimensional periodic boundary conditions are used to avoid the surfaces effects. In order to obtain Cu-rich clusters, simulation systems are relaxed in 2×10^5 steps with NPT ensemble. Subsequently, simulations are carried out in 2.5×10^8 steps with NVT ensemble under the same temperature and pressure conditions. The MD time step is 2 fs. The specific simulation parameters are presented in Table 1. To visualize the formation process of Cu cluster, OVITO[43] and VMD[44] are used.

Table 1. General conditions of the molecular dynamics (MD) simulations.

Parameter	Simulation value
Alloy	Fe–1.24%Cu–0.62%Ni alloy
Potential of alloy	EAM
Model size	$35a \times 35a \times 35a$ ($a = 2.855$ Å)
Boundary condition	PPP
MD time step	2 fs
Vacancy concentration	0.1%, 0.5%, 1.0%

In the present work, the radial distribution function (RDF) is calculated to indicate the phase transition process. The mean square displacement (MSD) of Cu atoms is calculated to indicate the diffusion process. The MSD is defined by the following equation:[27]

$$\left\langle R^2(t)\right\rangle = \frac{\sum_{j}^{N_{\mathrm{Cu}}}\left[r_j(t) - r_j(0)\right]^2}{N_{\mathrm{Cu}}}, \tag{1}$$

where t is the simulation time, r_j (0) is the initial position of the j-th atom, $r_j(t)$ is the position at times t of the j-th atoms, $\langle R^2(t)\rangle$ is MSD, and N_{Cu} is the total number of Cu atoms in the system.

The diffusion coefficient D^* (at a given temperature and vacancy concentration) in α-Fe can be obtained from the following equation:[45]

$$D^* = \frac{\left\langle R^2(t)\right\rangle}{6t}. \tag{2}$$

In order to analyze the evolution of Cu cluster, the size and atom number of Cu cluster are determined based on the study of Miller.[46] The cutoff distance for the interatomic potential is equal to 4.0 Å. This value is determined by the third nearest neighbor interaction of Cu atom. That is to say, atoms whose interatomic distance is less than 4.0 Å are considered to have interatomic interactions and form Cu cluster. Cu_x is defined as the number of Cu atoms contained in a Cu cluster, which is equal to or greater than x. $\mathrm{Cu}_{\mathrm{max}}$ represents the number of Cu atoms contained in the largest cluster and $\mathrm{CuNi}_{\mathrm{max}}$ represents the atom number in maximum co-composed cluster of Cu atoms and Ni atoms.

3. Results and discussion

3.1. Effect of Ni atoms on Cu diffusion in Fe–Cu–Ni ternary alloy

The MSDs of Fe, Cu, and Ni atoms in Fe–Cu–Ni ternary alloy with a vacancy concentration of 0.1% at 773 K are shown in Fig. 1(a). It can be obviously found that the MSD of Cu atoms is much greater than those of Ni and Fe atoms, which implies that Cu atoms of Fe–Cu–Ni alloy have longer distance diffusion capability. Therefore, Cu atoms are the main component of cluster in Fe–Cu–Ni ternary alloy. The MSDs of Fe and Ni atoms in Fe–Ni binary alloy can be seen in Fig. 1(b). The MSDs of Ni and Fe atoms, different from those in Fig. 1(a), are essentially coincident. While the MSD of Ni atoms in Fig. 1(a) is higher than that of Fe atoms in Fig. 1(a) and Ni atoms in Fig. 1(b), we can conclude that Cu atoms can promote the proliferation of Ni atoms, which fits well to the results of Wei *et al.*[47]

The Cu MSD curves in Fe–Cu–Ni and Fe–Cu alloys with a vacancy concentration of 0.1% are shown in Fig. 2. Obviously, between points A and B, the value of Cu MSD in Fe–Cu–Ni ternary alloy is larger than that in Fe–Cu binary alloy, which indicates that Ni atoms accelerate Cu diffusion in ferric alloy. Moreover, in the respect of energy, the cohesive energies of Cu and Ni are 3.49 eV/atom and 4.44 eV/atom,[48]

respectively, which means that the Cu clusters formed in Fe–Cu–Ni alloy are more stable and more easy to grow into larger clusters due to the addition of Ni atoms.

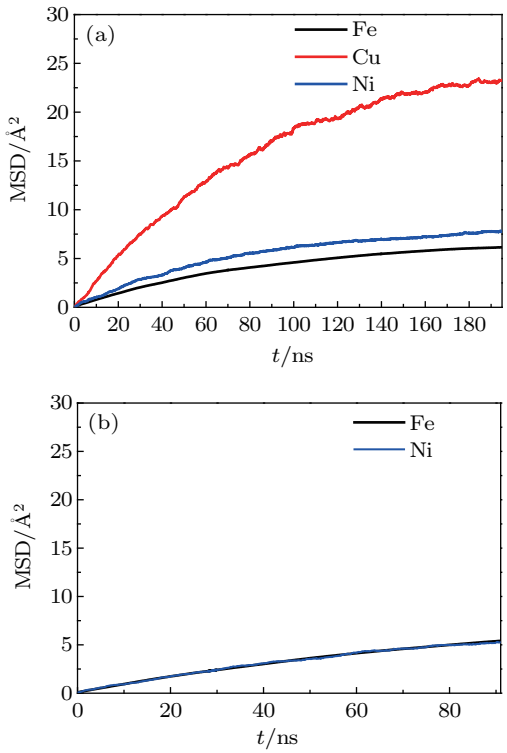


Fig. 1. (color online) (a) MSDs of Fe, Cu, Ni atoms in Fe-1.24% Cu-0.62% Ni alloy with vacancy concentration of 0.1%, (b) MSDs of Fe, Ni atoms in Fe-0.62% Ni alloy with vacancy concentration of 0.1%.

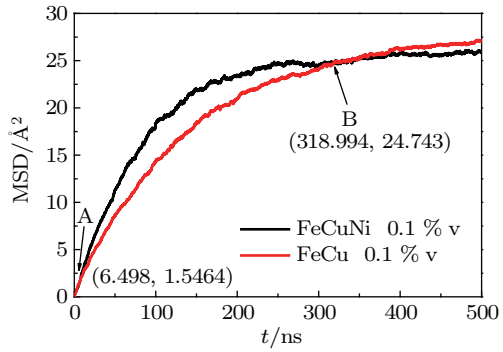


Fig. 2. (color online) MSDs of Cu atoms in Fe-1.24% Cu-0.62% Ni and Fe-1.24% Cu alloys with vacancy concentration of 0.1%.

From the above discussion, we know that Cu atoms and Ni atoms interact with each other during the formation of Cu precipitates in Fe matrix. So we divide the Cu diffusion into three stages according to different interaction behaviors between Cu and Ni atoms. Stage I is for the free diffusions of Cu and Ni atoms, stage II is for the mutual promotion between Ni and Cu atoms, and stage III is for the inhibition of Ni atoms on Cu diffusion. These three stages correspond to 0–A segment, A–B segment, and B afterward segment in Fig. 2. In 0–A segment, the Cu MSD curves in these two alloys are substantially coincident. In A–B segment, it can be clearly found that the addition of Ni atoms can significantly increase the Cu MSD value. Thus, Ni atoms can promote Cu precipitation obviously at the initial stage, which fits well to the results of Al-Motasem *et al.*[34,49] From B afterward segment, it can be found that the Cu MSD value of 0.1% v Fe–Cu–Ni alloy is less than that of 0.1% v Fe–Cu alloy. This phenomenon reveals that Ni atoms have a temporal delay effect on Cu precipitation when the simulation is carried out to a certain time, which is 318.994 ns in this paper. In other words, we conclude that Ni atoms accelerate Cu precipitation at the nucleation stage, and inhibit Cu precipitation at the coarsening stage.

The composition of Cu precipitates during ageing has been debated for a long time. The classical theory of nucleation predicts the formation of precipitates with a composition close to the equilibrium one, i.e., the formation of almost pure Cu cluster. In order to give an in-depth insight into the influence of Ni on the formation of Cu cluster, the specific configurations of Cu and Ni atoms are shown in Fig. 3. The formation and annihilation of the clusters, which form in the equilibrium process, are all undergoing in the whole simulation process. Cu and Ni atoms gather into small clusters, and then these small clusters grow into big ones, acting as precipitation precursors. The acceleration of Ni atoms on Cu diffusion has been discussed before.[37] In this part, we explain the inhabitation of Ni atoms on Cu diffusion. Therefore, the visualization patterns of Cu diffusion after 200 ns have been chosen. Additionally, Fe atoms are not displayed for clarity. According to the study of Isheim *et al.*,[50] as the number of solute atoms in one cluster is equal to seven, the number of atoms in this cluster is more than ten in RPV steel. Therefore, the clusters which we discuss in this part are not small. Furthermore, the cluster analysis in this simulation has carefully performed to avoid detecting the statistical fluctuations of solute atom concentration.

Figures 3(a) and 3(b) show the snapshots at 200 ns and 220 ns, respectively. These two moments are at stage II of Cu diffusion. Small clusters coalesce into big ones by the interaction between Cu–Cu and Cu–Ni bonds. Obviously Ni atoms are located at the connection positions of three Cu clusters, and then the three small Cu clusters merge into big ones as shown in region I of Fig. 3(a). With the simulation process progressing, Cu clusters gradually grow up. Accordingly, the above process can be described as large Cu clusters growing from small and subcritical clusters.

From region II through Figs. 3(a)–3(d), it can be seen that the structure of Cu cluster is basically stable and the atoms of some Cu clusters increase up to a certain number. Ni atoms are rejected from the core to interface[47] and the stable structure of Cu cluster presents a similar spherical appearance, where Ni atoms scatter around the Cu core. These configurations are core-shell structure,[34,36,37,51] which is due to the dynamic migration of Ni atoms. Furthermore, Ni atoms have a strong tendency toward forming Fe–Ni bonds in Fe–Cu–Ni ternary

alloy,[52] and gradually Ni atoms are excluded from the Cu cluster to the interface between the Cu cluster and Fe-matrix over time.

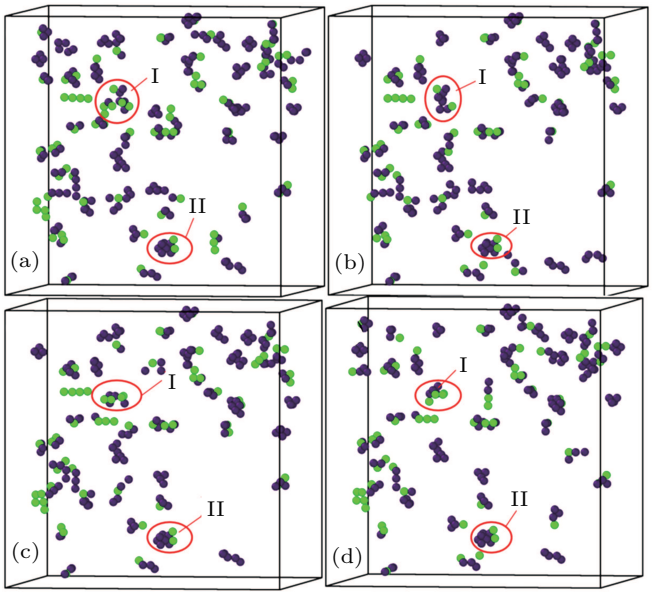


Fig. 3. (color online) Formation of Cu clusters of Fe-1.24% Cu-0.62% Ni alloys with vacancy concentration of 0.1% (Fe atoms are not displayed for clarity.) at (a) 200 ns, (b) 220 ns, (c) 300 ns, (d) 340 ns.

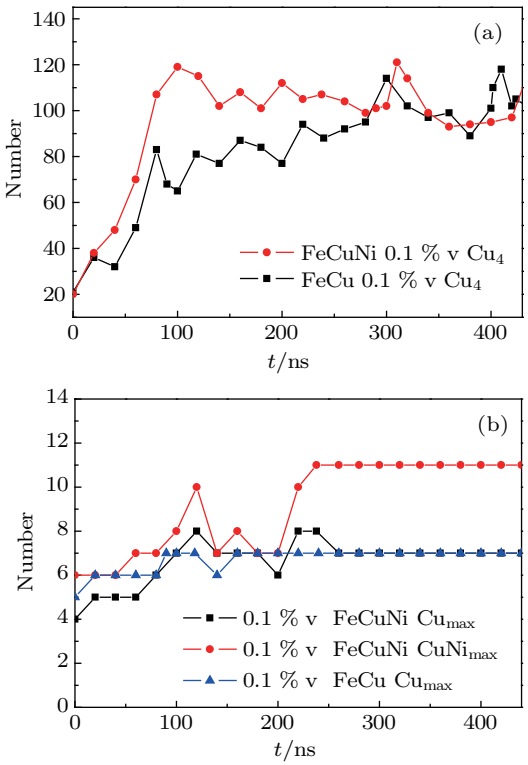


Fig. 4. (color online) (a) Variations of Cu_4 number with ageing time in Fe-1.24% Cu-0.62% Ni alloy and Fe-1.24% Cu alloy with vacancy concentration of 0.1%, (b) variations of Cu_{max} and $CuNi_{max}$ number with ageing time in Fe-1.24% Cu-0.62% Ni alloys and Fe-1.24% Cu alloys with vacancy concentration of 0.1%.

Ni segregates into the core region of the precipitate at the initial formation stage and can be pushed away from the core towards the interface of the precipitates for the following growth stage. This is consistent with phase field,[53] first principles[54] and Langer–Schwartz[38] simulations. These phenomena were also observed experimentally.[51,55]

To compute the size of precipitate in the simulations, we only take into account clusters, in which the number of solute atoms is more than four, connected with at least one nearest neighbor bond. The exact value of this critical size does not significantly affect the results for time above 1 fs — it does not change, in particular, the comparison with experimental results. Figure 4 shows the changes of the numbers of Cu_4, Cu_{max}, and $CuNi_{max}$ with time in Fe–Cu–Ni ternary alloy and Fe–Cu binary alloy under a vacancy concentration of 0.1%. It can be illustrated that the Cu_{max} curves are unstable and gradually increase along stage I and stage II, and the value of Cu_{max} becomes stable when the Cu diffusion enters into stage III shown in Fig. 4(b). It can be concluded that Ni atoms promote Cu precipitate in the early stages of ageing, and the number of Cu_4 in 0.1% v Fe–Cu–Ni alloy is more than that in 0.1% v Fe–Cu alloy as indicated from Fig. 4(a). The values of Cu_{max} in 0.1% v Fe–Cu–Ni alloy and 0.1% v Fe–Cu alloys shown in Fig. 4(b) illustrate that there is no significant effect of Ni atoms on Cu_{max} at the stable stage after 260 ns in this simulation.

3.2. Effect of vacancy concentration on Cu diffusion in Fe–Cu–Ni ternary alloy

The MSD curves of Cu with three different vacancy concentrations in Fe–Cu–Ni ternary alloys are shown in Fig. 5. Corresponding intersections of each curve are described as points A, B, C, and D with coordinates presented in Table 2. Before point A, the diffusion coefficients of Cu in 1.0% v Fe–Cu–Ni alloy, 0.5% v Fe–Cu–Ni alloy, and 0.1% v Fe–Cu–Ni alloy are $D_{\mathrm{FeCuNi1.0\%v}} = 0.261 \times 10^{-9}$ cm^2/s, $D_{\mathrm{FeCuNi0.5\%v}} = 0.211 \times 10^{-9}$ cm^2/s, and $D_{\mathrm{FeCuNi0.1\%v}} = 0.034 \times 10^{-9}$ cm^2/s, respectively, which lead to a ratio of 8:6:1. Hence it can be inferred that the higher the vacancy concentration, the greater the diffusion rate of Cu atoms at the early stage of ageing is. After point A, the slopes of Cu MSD curves become sharply lower with high vacancy concentration, for which the reason is that with more vacancies in the initial model, it is more likely to form vacancy clusters.[42] Furthermore, from the study of Ludwig *et al.*,[16] the vacancy precipitates more easily in Cu cluster than in α-Fe. Frédéric Soisson *et al.*[42] have also observed that the trapping of the vacancy vibrates dramatically during the Cu precipitation in pure iron. From then on, Cu diffusion in Fe–Cu–Ni alloys decreases with vacancy density increasing. In other words, vacancy dominantly precipitates in higher vacancy concentration during ageing, which corresponds with the previous study.[56] Between points B and D, it can be found that the MSD value of Cu is larger in lower vacancy concentration. This difference can be explained by the

vacancy–vacancy interaction, i.e., the mono-vacancies rapidly aggregate into vacancy clusters, which leads to a decrease in Cu diffusion. In general, the diffusions of Cu and Ni atoms in α-Fe occur via a vacancy diffusion mechanism.[39,57] According to the comparison of MSD tendency in Fe–Cu–Ni alloy between the vacancy concentration of 0.1% and 1.0%, 0.1%, and 0.5%, the result is substantially similar to that obtained by Osetsky *et al.*[39] But there is an intersection which appears after 150 ns in this simulation and is marked as point D in Fig. 5. It can be traced that the vacancy concentration gap between 0.5% and 1.0% is small and the atomic configurations are more stable after point B, so the trend-proliferation of Cu MSDs becomes closer with ageing time and the intersection point D appears at 163.856 ns. It can be inferred that the fluctuation of Cu MSDs around point D having a similar tendency is due to the influence of mono-vacancy concentration. Through the comparison between Cu MSDs in 0.5% v and 1.0% v, after point D, the Cu MSDs increase with vacancy concentration increasing For that, the Cu MSD for mono-vacancy concentration with a 1.0% vacancy concentration is slightly higher than that with a 0.5% vacancy concentration.

Table 2. Intersections of Cu MSDs with different vacancy concentrations of Fe–1.24%Cu–0.62% Ni alloys.

Point	Coordinates (t/ns, MSD/Å^2)
A	(13.498, 7.9611)
B	(50.298, 11.3806)
C	(53.598, 11.8157)
D	(163.856, 15.3916)

In order to reveal what has happened more clearly around intersections with different vacancy concentrations of Fe–Cu–Ni alloys, $g_{\mathrm{Cu-Cu}}(r)$s are calculated and shown in Fig. 6, which correspond to 8 moments (0 ns, 10 ns, 20 ns, 40 ns, 60 ns, 140 ns, 180 ns, 200 ns) before and after each intersection in Fig. 5.

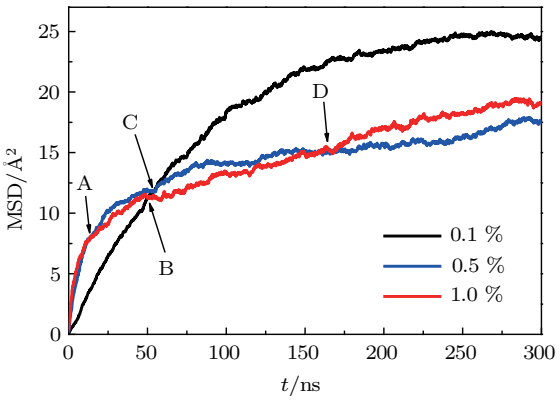


Fig. 5. (color online) Time-dependent MSDs of Cu atoms in Fe–1.24%Cu–0.62% Ni alloys with vacancy concentration of 0.1%, 0.5%, and 1.0%.

Figure 6(a) describes the $g_{\mathrm{Cu-Cu}}(r)$ with different vacancy concentrations at 0 ns. As reflected in Fig. 6(a), all peaks of $g_{\mathrm{Cu-Cu}}(r)$ of Fe–Cu–Ni alloys with different vacancy concentrations are homogeneous. It indicates that Cu atoms in Fe–Cu–Ni alloys distribute uniformly at 0 ns. By comparing Fig. 6(b) with Fig. 6(c), conclusion can be drawn that the degree of Cu aggregation in 0.5% v Fe–Cu–Ni alloy is more significant than that in 1.0% v Fe–Cu–Ni alloy after 13.498 ns. The comparison between Figs. 6(d) and 6(e) illustrates that the degrees of Cu aggregation with different vacancy concentrations are changed around point C in Fig. 5. From Fig. 6(e), it can be obtained that the degree of Cu aggregation in 0.1% v Fe–Cu–Ni alloy is highest at 60 ns. By comprehensive comparison among curves of $g_{\mathrm{Cu-Cu}}(r)$ in Figs. 6(f)–6(h), the extent of Cu concentration changes little with vacancy concentration around 163.856 ns. And with the ageing time increasing to 200 ns, the $g_{\mathrm{Cu-Cu}}(r)$ value of 1.0% v Fe–Cu–Ni alloy is still highest. All these results are in good agreement with the MSD curves in Fig. 5.

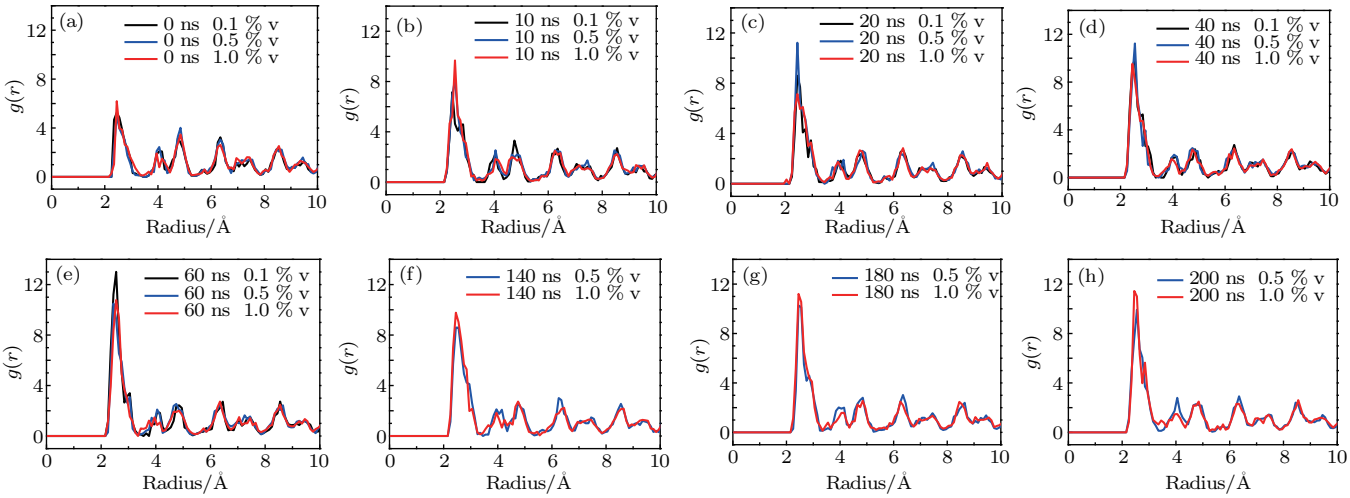


Fig. 6. (color online) Partial pair distribution functions $g_{\mathrm{Cu-Cu}}(r)$ of Fe-1.24% Cu-0.62% Ni alloys for different time with different vacancy concentrations.

The Cu_4, Cu_{max}, and $CuNi_{max}$ in Fe–Cu–Ni alloys with different vacancy concentrations are shown in Fig. 7. From Fig. 7(a), two trends can be revealed. Before point A, the larger the vacancy concentration in Fe–Cu–Ni alloy, the more the Cu_4 precipitates. After point A, the tendencies of the two curves are obviously different at first, and become the same at the end of this simulation. Fig. 7(b) shows that between the two different vacancy concentrations in Fe–Cu–Ni alloys, Cu_{max} changes distinguishably at the early stage of Cu diffusion, and reaches consistence at the later stage. Meanwhile, $CuNi_{max}$ and Cu_{max} have the similar tendencies and $CuNi_{max}$ becomes the same at the end of the simulation. Hence, it can be concluded that the effect of vacancy concentration on Cu cluster is obvious at early ageing stage, but insufficient at later stage.

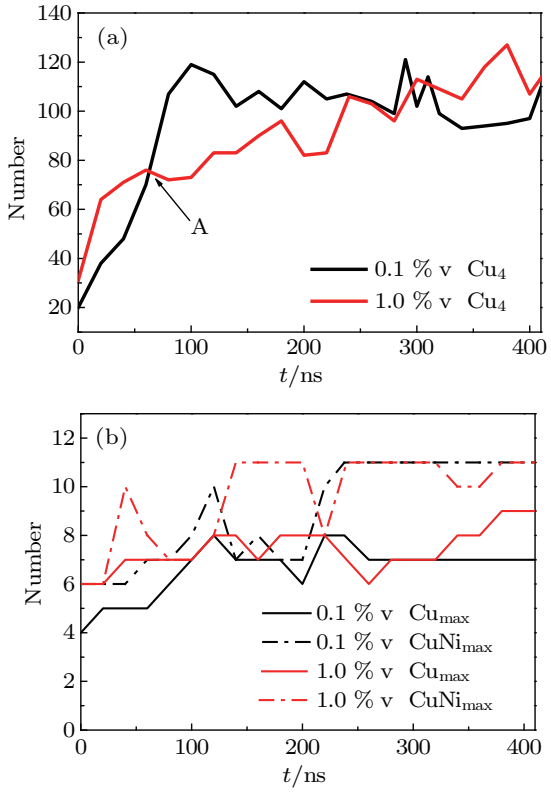


Fig. 7. (color online) (a) Time-dependent Cu_4 in Fe–1.24%Cu–0.62% Ni alloys with different vacancy concentrations, and (b) time-dependent Cu_{max} and $CuNi_{max}$ in Fe–1.24%Cu–0.62% Ni alloys with different vacancy concentrations.

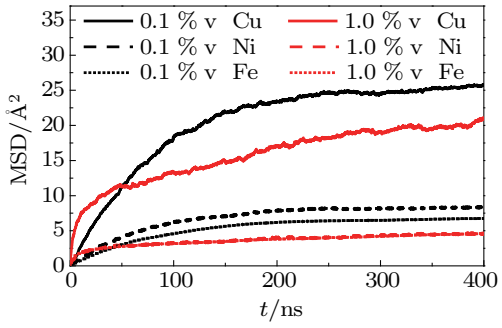


Fig. 8. (color online) Time-dependent MSDs of Cu, Ni, and Fe atoms in Fe–1.24%Cu–0.62% Ni alloys with vacancy concentrations of 0.1% and 1.0%.

From Fig. 8, it can be found that the MSDs of Ni atoms and Fe atoms coincide almost perfectly when the vacancy concentration increases to 1.0%, which is similar to the MSDs of Ni and Fe atoms in Fe–Ni binary alloy shown in Fig. 1(b). Therefore, it can be inferred that the promotion of Cu on Ni decreases when the vacancy concentration increases to 1.0%.

Figure 9 illustrates the Cu MSD tendencies of Fe–Cu–Ni and Fe–Cu alloys with a vacancy concentration of 1.0%. The intersection between Fe–Cu–Ni and Fe–Cu alloys with 1.0% v appears at point A. Before point A, the two curves are essentially coincident. By comparing with Fig. 2, which is for the same alloys but different vacancy concentrations, it is clearly observed that the t-value of point A in Fig. 9 is more than seven times that in Fig. 2. Thus, it can be inferred that the influence of Ni on Cu diffusion decreases with vacancy concentration increasing. Or the interaction between Ni and Cu decreases when the vacancy concentration increases up to 1.0%.

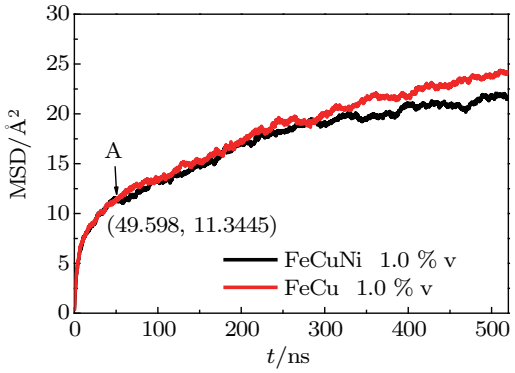


Fig. 9. (color online) Time-dependent MSDs of Cu in Fe–1.24%Cu–0.62% Ni and Fe–1.24%Cu alloys with vacancy concentration of 1.0%.

4. Conclusions and perspectives

Based on molecular dynamics simulation, the influence of vacancy concentration and Ni solute atoms on Cu precipitate in Fe–1.24%Cu–0.62% Ni during ageing are investigated. Ni atoms accelerate Cu precipitation at the nucleation stage, while inhibit Cu precipitation at the coarsening stage. The atom number and size of Cu cluster correspondingly increase with vacancy concentration from 0.1% to 1.0%. As the vacancy concentration increases to 1.0%, Ni atoms have little effect on the process of Cu diffusion compared with vacancy concentration.

Acknowledgment

All the computations were performed on the high performance computing platform of Shanghai University.

References

[1] Odette G and Lucas G 2001 *JOM* **53** 18
[2] Nagai Y, Tang Z, Hassegawa M, Kanai T and Saneyasu M 2001 *Phys. Rev. B* **63** 134110
[3] Dubuisson P, Schill R, Hugon M, Grislin I, Seran J, Nanstad R, Hamilton M, Garner F and Kumar A 1999 *ASTM STP* **1325** 882

[4] Yu X M and Zhao S J 2013 *Acta Metall. Sin.* **49** 569 (in Chinese)
[5] Yang G, Wang J X and Yang M X 2012 *T. Mater. Heat Treat.* **33** 51
[6] Liu Q D, Gu J F and Li C W 2014 *J. Mater. Res.* **29** 950
[7] Liu Q D and Zhao S J 2013 *Metall. Mater. Trans. A* **44** 163
[8] Fine M, Liu J and Asta M 2007 *Mater. Sci. Eng. A* **463** 271
[9] Monzen R, Iguchi M and Jenkins M 2000 *Philos. Mag. Lett.* **80** 137
[10] Osamura K, Okuda H, Takashima M, Asano K and Furusaka M 1993 *Mater. Trans. JIM* **34** 305
[11] Othen P, Jenkins M and Smith G 1994 *Philos. Mag. A* **70** 1
[12] Liu F, Zhou B, Peng J C and Wang J A 2013 *Acta Metallurgica Sinica* **26** 707
[13] Kamada Y, Takahashi S, Kikuchi H, Kobayashi S, Ara K, Echigoya J, Tozawa Y and Watanabe K 2009 *J. Mater. Sci.* **44** 949
[14] Ghosh A, Mishra B, Das S and Chatterjee S 2005 *Metall. Mater. Trans. A* **36** 703
[15] Primig S, Stechauner G and Kozeschnik E 2017 *Steel Res. Int.* **88**
[16] Ludwig M, Farkas D, Pedraza D and Schmauder S 1998 *Modell. Simul. Mater. Sci. Eng.* **6** 19
[17] Molnar D, Niedermeier C, Mora A, Binkele P and Schmauder S 2012 *Continuum Mech. Thermodyn.* **24** 607
[18] Molnar D, Mukherjee R, Choudhury A, Mora A, Binkele P, Selzer M, Nestler B and Schmauder S 2012 *Acta Mater.* **60** 6961
[19] Seko A, Odagaki N, Nishitani S R, Tanaka I and Adachi H 2004 *Mater. Trans.* **45** 1978
[20] Soisson F, Barbu A and Martin G 1996 *Acta Mater.* **44** 3789
[21] Cerezo A, Hirosawa S, Rozdilsky I and Smith G 2003 *Philos. Trans. R. Soc. London, Ser. A* **361** 463
[22] Monasterio P, Wirth B and Odette G 2007 *J. Nucl. Mater.* **361** 127
[23] Blackstock J and Ackland G 2001 *Philos. Mag. A* **81** 2127
[24] Ackland G, Bacon D, Calder A and Harry T 1997 *Philos. Mag. A* **75** 713
[25] Domain C and Becquart C 2001 *Phys. Rev. B* **65** 024103
[26] Liu J Z, Van De Walle A, Ghosh G and Asta M 2005 *Phys. Rev. B* **72** 144109
[27] Marian J, Wirth B, Odette G and Perlado J 2004 *Comput. Mater. Sci.* **31** 347
[28] Gao N, Wei K F, Zhang S X and Wang Z G 2012 *Chin. Phys. Lett.* **29** 096102
[29] Bergner F, Lambrecht M, Ulbricht A and Almazouzi A 2010 *J. Nucl. Mater.* **399** 129
[30] Nagai Y, Takadate K, Tang Z, Ohkubo H, Sunaga H, Takizawa H and Hasegawa M 2003 *Phys. Rev. B* **67** 224202
[31] Xu Q, Yoshiie T and Sato K 2006 *Phys. Rev. B* **73** 134115
[32] Miller M, Wirth B and Odette G 2003 *Mater. Sci. Eng. A* **353** 133
[33] Zhang C, Enomoto M, Yamashita T and Sano N 2004 *Metall. Mater. Trans. A* **35** 1263
[34] Al-Motasem A, Posselt M and Bergner F 2011 *J. Nucl. Mater.* **418** 215
[35] Bonny G, Pasianot R C, Castin N and Malerba L 2009 *Philos. Mag.* **89** 3531
[36] Osamura K, Okuda H, Asano K, Furusaka M, Kishida K, Kurosawa F and Uemori R 1994 *ISIJ Int.* **34** 346
[37] Zhu L S and Zhao S J 2014 *Chin. Phys. B* **23** 063601
[38] Zhang C and Enomoto M 2006 *Acta Mater.* **54** 4183
[39] Osetsky Y N and Serra A 1997 *Philos. Mag. A* **75** 1097
[40] Wang Y, Hou H Y, Liu X B, Wang R S and Wang J T 2012 arXiv preprint arXiv: 1212.6900
[41] Plimpton S 1995 *J. Comput. Phys.* **117** 1
[42] Soisson F and Fu C C 2007 *Phys. Rev. B* **76** 214102
[43] Stukowski A 2009 *Modell. Simul. Mater. Sci. Eng.* **18** 015012
[44] Humphrey W, Dalke A and Schulten K 1996 *J. Mol. Graphics* **14** 33
[45] Ju Y Y, Zhang Q M, Gong Z Z and Ji G F 2013 *Chin. Phys. B* **22** 083101
[46] Miller M K 2012 *Atom probe tomography: analysis at the atomic level*, (Springer Science & Business Media)
[47] Wei X R abd Zhao S J 2013 *Shanghai Metals* **35** 5-8+35
[48] Kittel C 2004 *Introduction to Solid State physics* (Wiley)
[49] Al-Motasem A, Posselt M, Bergner F and Birkenheuer U 2011 *J. Nucl. Mater.* **414** 161
[50] Isheim D, Gagliano M S, Fine M E and Seidman D N 2006 *Acta Mater.* **54** 841
[51] Pareige P, Russell K and Miller M 1996 *Appl. Surf. Sci.* **94** 362
[52] Murthy A S, Medvedeva J E, Isheim D, Lekakh S L, Richards V L and Van Aken D C 2012 *Scr. Mater.* **66** 943
[53] Koyama T, Hashimoto K and Onodera H 2006 *Mater. Trans.* **47** 2765
[54] Xie Y P and Zhao S J 2012 *Comput. Mater. Sci.* **63** 329
[55] Hyde J, Sha G, Marquis E, Morley A, Wilford K and Williams T 2011 *Ultramicroscopy* **111** 664
[56] Schober H, Petry W and Trampenau J 1992 *J. Phys.: Condens. Matter* **4** 9321
[57] Vincent E, Becquart C and Domain C 2006 *J. Nucl. Mater.* **351** 88